Tunable One-Dimensional Silver−Silica Nanopeapod Architectures

ARTICLE *in* THE JOURNAL OF PHYSICAL CHEMISTRY B · MAY 2006

Impact Factor: 3.3 · DOI: 10.1021/jp0603076 · Source: PubMed

2 AUTHORS, INCLUDING:

Simona E. Hunyadi Murph
Savannah River National Laboratory
63 PUBLICATIONS **2,763** CITATIONS

SEE PROFILE

Tunable One-Dimensional Silver−Silica Nanopeapod Architectures

Simona E. Hunyadi and Catherine J. Murphy*

Department of Chemistry and Biochemistry, University of South Carolina, 631 Sumter Street, Columbia, South Carolina 29208

Received: January 16, 2006; In Final Form: March 1, 2006

Silica-coated silver nanowires can be chemically treated to produce a "peapod" architecture in which silver peas are embedded in silica pods. The silver "pea" dimension and interparticle spacings are controllable down to ∼50 nm. This architecture is potentially useful for chemical sensing, plasmonic, or catalytic applications.

Introduction

Ordered arrays of metal nanoparticles hold great promise for many applications.[1−4] Recent theoretical and experimental work suggests that one-dimensional metal nanoparticle arrays can be utilized to transport electromagnetic energy ("plasmonics").[5−7] Maier et al. demonstrated that periodic arrays of metallic structures (specifically, lithographically prepared silver nanorods) embedded in dielectric media are able to guide and modulate light transmission (even through corners and tee structures) in a regime dominated by near-field coupling.[6] In the case of metallic nanoparticles, the mechanism of communication is the surface plasmon modes, which are a collective oscillation of conduction band electrons whose intense local fields may lead toward precise, photoinitiated processes in nanostructured arrays.[5−7] Molecules that are near nanoscale metal particles or surfaces experience greatly enhanced Raman signals, principally due to the enormous electric fields created when plasmon modes are activated by absorption of visible light.[8] Nanoscale junctions between metal nanoparticles provide larger surface-enhanced Raman scattering signals for molecules that reside there compared to that of single particles.[8−10] For example, Schatz[10] describes special silver nanoparticle array structures that lead to exceptionally large electromagnetic field enhancements ($|\mathbf{E}|^2 > 10^7$) at specific locations in the structure, thus providing a purely electromagnetic mechanism for producing single-molecule surface-enhanced Raman scattering (SERS) enhancements $>10^{13}$ compared to that of conventional Raman scattering.

Precise assembly of nanoscale metal particles into optimized geometries for either plasmonics or chemical sensing via SERS is an ongoing challenge. Nanorods are thought to be superior to nanospheres for SERS, especially if the molecule to be detected is located at the tips of the rods rather than the sides.[8−10] One desired geometry is a nanoscale "beads on a string" or "peapod" architecture, in which nanoscale metal "peas" are separated by nanoscale distances. To create nanopeapod architectures, various techniques have been used in the literature. For example, electron beam lithography[6,11] or insertion of particles into preformed structures[12,13] provide good control over particle placement, but are costly and time-consuming. Carbon nanotubes also can serve as templates for the formation of metal nanoparticle assemblies.[13,14] Keating et al.[15] developed a wet-chemical method for fabricating linear chains of Au and Ag nanoparticles by selectively etching alternating segments from striped metal nanowires that had been electrodeposited in nanoporous membranes. After removal from the membrane, wires were coated with SiO_2, and selective etching revealed the nanoparticle chains. However, removal of the template is required, which might lead to the disturbance of the architecture. Scaling up the production of such nanomaterials is likely to be difficult using the hard template approach.

In this report, we present a convenient and straightforward wet-chemical route to produce "nanopeapod" architectures in which silver "peas" are embedded in a silica "pod." The dimensions of the peas, and their spacing within the pod, are controllable on the nanoscale.

Experimental Section

Materials and Methods. Silver nitrate ($AgNO_3$, 99%), sodium silicate solution (∼27% SiO_2 in water), 3-mercaptopropyltrimethoxysilane (MPTMS, 95%), and ammonia (NH_3, 25%, 14 N) aqueous solution were all from Sigma-Aldrich and used as received. Deionized water was used throughout the experiments. Transmission electron microscopy was performed with a Hitachi 8000 transmission electron microscope on copper grids operating at 200 kV. UV−Vis spectroscopy was performed on a Cary 500 Scan UV−vis−NIR spectrophotometer.

Synthesis of Ag Nanowires. Silver nanowires were prepared in water, in the absence of surfactant or polymer and without externally added seed crystallites, as described elsewehere.[16] Basically, a typical synthesis requires the combination of two silver ion solutions. The first solution contained 100 mL of deionized water, 1.5 μL of 0.1 M NaOH, and 40 μL of 0.1 M $AgNO_3$. This solution was brought to a boil with rapid stirring. Then, 5 mL of 0.01 M trisodium citrate was added to it and then boiled for another 10 min. At the same time, a second solution containing 150 mL of deionized water, 1.5 μL of 0.1M NaOH, and 20 μL of 0.1M $AgNO_3$ was brought to a boil. Finally, the second solution was added to the initial one, and the mixture was allowed to boil for 60 min.

Synthesis of Ag@SiO_2. Different volumes (5 mL, 10 mL, 20 mL, 25 mL, 30 mL, 40 mL, 50 mL, 60 mL, 70 mL, or 80 mL) of 0.5 mM 3-mercaptopropyltrimetoxysilane (MPTMS) solution was added to a 1-mL aliquot of silver nanowire solution. The solutions were then stirred for 20 min to ensure that

* To whom correspondence should be addressed. E-mail: murphy@mail.chem.sc.edu.

10.1021/jp0603076 CCC: $33.50
Published on Web 03/23/2006

SCHEME 1. Silica Coating Process[a]

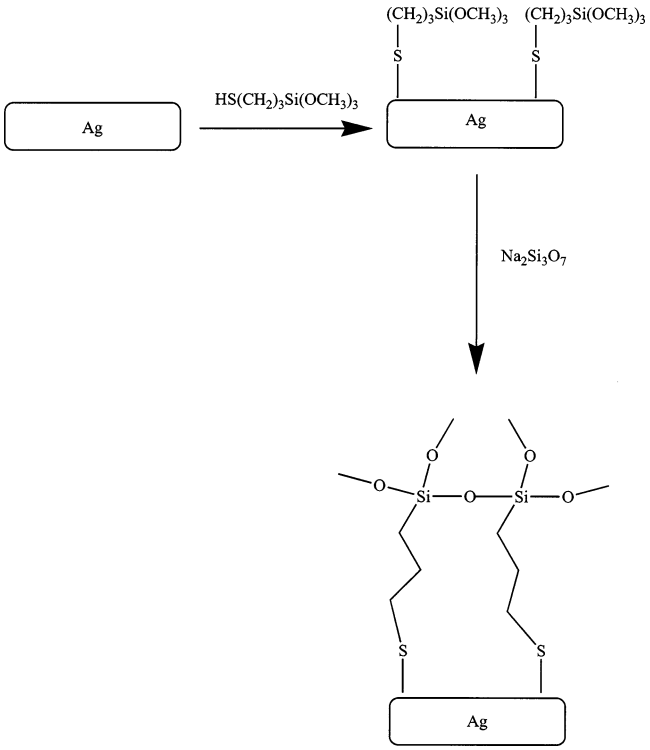

[a] MPTMS is linked through the sulfur to the silver nanowire surface, leaving free trimethoxysilane groups facing the solvent. Addition of sodium silicate produces silica, SiO_2.

MPTMS was bound to the silver nanowire. Then different volumes (2 μL, 5 μL, or 10 μL) of sodium silicate ($Na_2O(SiO_2)_3$, a 0.252 M stock solution) was added, and the stirring was continued for another 20 min. The solution was left overnight to allow formation of a uniform layer of silica. The next day, coated nanoparticles were separated from the reaction medium by centrifugation (5000 rpm for 15 min) and redispersion into deionized water. The silica thickness was easily controlled from ∼10 up to ∼150 nm with a homogeneous coating over the entire surface of the nanowire, depending on initial precursor concentrations. When the concentration exceeded 8.08 mM MPTMS, the silica shell became inconsistent and nonuniform. The control experiment to grow SiO_2 on Ag nanowires without the MPTMS linker was performed by following the same steps. Typically, different volumes (5 μL, 10 μL, 20 μL, or 25 μL) of 0.252 M sodium silicate were directly put into solutions of Ag nanowires for 20 min under the same conditions. During the control experiment, the maximum shell thickness achieved was on average 6.5 nm, independent of the initial concentration of the sodium silicate.

Synthesis of Nanopeapods (Ammonia Dissolution Treatment). The formation of Ag−silica nanopeapods was achieved by keeping the nanocomposite materials (Ag coated with silica) in an ammonia solution (25%, 14 N) for ∼1−2 days with a 20 min initial stirring time. We varied the initial stirring time from 0 min, 20 min, 2, 4, or 6 h. Regular peapods were formed only for the initial 20-min stirring condition. As the silica shell thickness increased, the immersion time in NH_3 required to produce the equally spaced nanopeapods varied also from 1 or 2 days. After that, ammonia was removed from the solution, and the nanopeapods were transferred for 3 days in DI to finish up the reaction between Ag and excess NH_3 present inside the system. The resultant nanopeapods architectures could be separated by centrifugation and redispersion into DI water.

Results and Discussion

Silver nanowires prepared by a seedless, surfactantless approach[16] were coated with a silica shell through an indirect coating method[17−19] that involved the use of a bifunctional linker, 3-mercaptopropyltrimethoxysilane ($HS(CH_2)_3Si(OCH_3)_3$, MPTMS), which binds to the Ag surface via the thiol group. A thin SiO_2 layer is subsequently grown on the MPTMS layer through a modified Stöber method (Scheme 1). The thickness of the silica shell can be controlled from approximately 9 to 150 nm (Figure 1) by adjusting the growth conditions.[20]

Growth of the silica shell was monitored via ζ potential measurements, transmission electron microscopy (TEM), and UV−visible absorption spectroscopy. The effective surface charge of the Ag nanowires before and after silica coating changed from -45 ± 4 to -57 ± 4 mV, for example, for a 50-nm silica shell thickness. The silver nanowires' original net negative charge is likely due to adsorbed hydroxide and citrate. Silica itself is well-known to bear a net negative charge in water due to deprotonated Si−OH surface groups; thus, the ζ potential measurements are in accord with the purported surface group. Transmission electron microscopy (Figure 1b−f) images show that the silica coating is uniform over the entire surface of each nanowire (up to a point), including both ends. The lengths of these silica nanotubes are determined by the original silver nanowires and could be as long as 14 μm.

By controlling the concentration of the silica precursors or the coating time, the thickness of the silica can be easily tuned. When the initial concentration of MPTMS varied from 0.54 up to 8.08 mM under our conditions, we were able to control the silica thickness from 9 to 150 nm. The thickness of the silica increased linearly as the concentration of the precursor increased (Figure 2). These results are similar to what others have observed for the coating of silica on metallic nanowires made by other

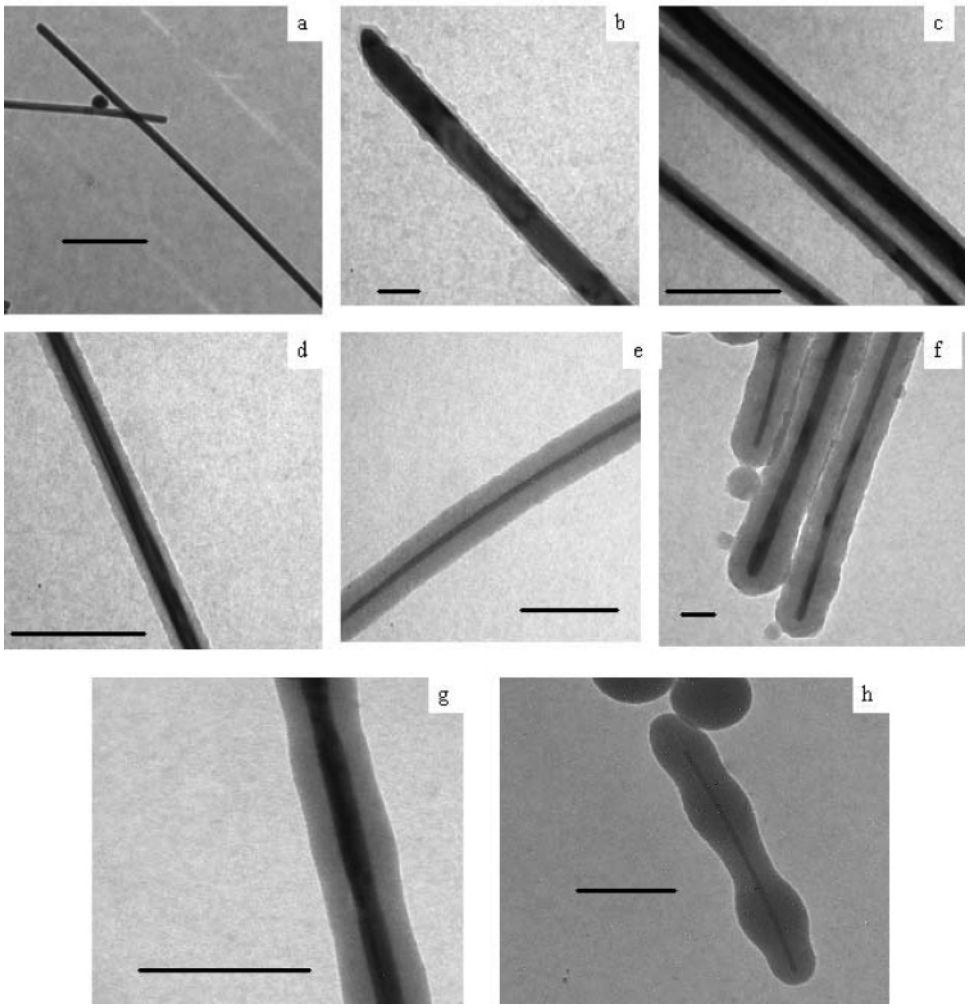

Figure 1. Representative transmission electron micrographs of silver nanowires and silica-coated silver nanowires. (a) TEM of silver nanowires as prepared by our solution method. Scale bar = 500 nm. (b−h) TEM images of different thicknesses of silica shells on silver nanowires; the shape of nanowire is preserved. Scale bar = 500 nm (b, c, d, e, g), 100 nm (f, h). Note that if the silica shell is too thick, the silica coating becomes inhomogeneous (h).

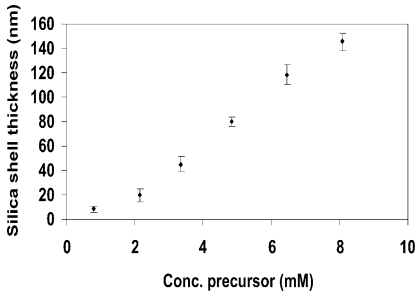

Figure 2. Dependence of silica shell thickness on the concentration of precursor.

means.[20b] As the concentration of the precursor exceeded 8.08 mM, we produced silica shells with an average thickness of 250 nm, but the shell became inconsistent and not uniform over the entire surface (Figure 1h). At the same time, many silica spheres were produced.

We have also found that MPTMS is important to make well-controlled layers of silica on silver. In a control experiment, in the absence of MPTMS, the sodium silicate solution was mixed directly with solutions of Ag nanowires under the same conditions. The silica shells produced with this direct coating approach were 5−10 nm in thickness, independent of sodium silicate concentrations from 1.26 up to 10.08 mM (Figure S1). This result confirms that MPTMS plays an important role in the coating process as a molecular "glue" at the interface of two inorganic materials.

The influence of the silica shell on the optical properties of the silver nanowires was studied with UV−vis spectroscopy (Figure 3). The transverse plasmon band at ∼400 nm appeared to red-shift with increasing silica shell thickness, consistent with theoretical predictions in the literature, which correlate this observation with an increase in the local dielectric constant surrounding the silver nanowires that is due to silica.[3−21] The longitudinal plasmon band is past 1400 nm and is also masked by water absorption. Some of the "absorbance" is due to scattering from these relatively large objects in solution; Figure 3e shows the optical spectra for hollow silica nanotubes without silver for comparison.

We have previously shown that silica-coated gold nanorods can be treated with cyanide, producing the soluble complex ion $[Au(CN)_2]^-$, which leaches out of the silica and leads to hollow silica nanotubes.[18a] An analogous reaction for silver can be carried out with aqueous ammonia, which produces the soluble complex ion $[Ag(NH_3)_2]^+$.[22] The TEM image (Figure 4a) shows that complete dissolution of the Ag core generates hollow silica nanotubes. Partial dissolution of the Ag core leads to surprisingly uniform "nanopeapods", in which silver peas are embedded in the silica pod (Figure 4b−f).

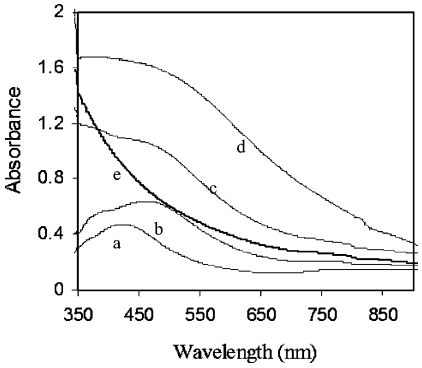

Figure 3. Absorption spectra of silver nanowires coated with various thickness of SiO_2. Silica shell thickness are (a) 0 nm, (b) 20 nm, (c) 46 nm, and (d) 80 nm. (e) Optical spectra of silica hollow nanotubes (46 nm shell thickness).

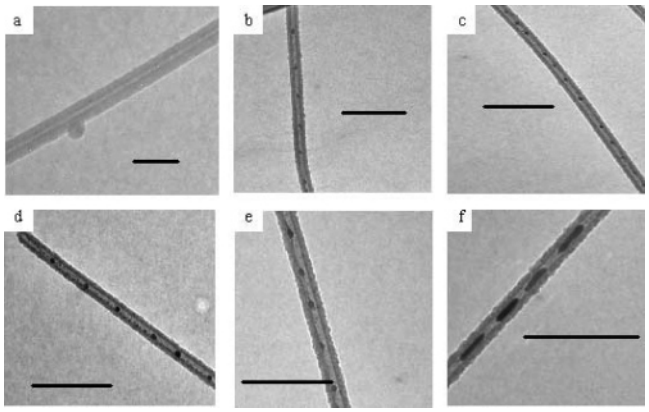

Figure 4. Transmission electron micrographs of silica-coated silver nanowires after treatment with aqueous ammonia. (a) TEM micrograph of hollow silica nanotubes made by complete dissolution of the silver core with aqueous ammonia. Scale bar = 100 nm. (b−f) TEMs of representative "peapod" architectures obtained under conditions of incomplete dissolution of the silver with ammonia, showing silver "peas" in silica "pods". Scale bars = 500 nm.

The embedded silver nanoparticle "peas" that have controlled lengths from ∼35 up to ∼240 nm, and controllable interpea distances from ∼350 to ∼25 nm, can be produced depending on reaction conditions and silica shell thickness. Parameters such as silica shell thickness, ammonia concentration, stirring time, etc. are all important. Without stirring, the silica shell becomes inhomogeneous upon ammonia treatment (Figure 5a). TEM experiments (Figure 5c, d) suggest that the reaction is initiated at the ends of the silver nanowires and percolates inward through the silica shell. Whether this is because the silica shell is more porous at the end, or the nanowires are more reactive at the ends, is unclear. We have reported preliminary electron diffraction evidence that the silver nanowires are crystallographically twinned, with a possibly strained arrangement of five tetrahedral {111} faces at the ends of the nanowires.[16] As the reaction to make silver nanowires evidently preferentially deposits metal at the ends of the nanorods (up to a point), we favor the notion that the ends are more reactive toward ammonia. However, the curvature of the silica shell at this point also could produce strain or defects in the silica caps at those points, and also influence the porosity at the ends.

The most unusual aspect of this process is that the ammonia, even though it may start reacting at the ends of the silver nanowires, does not keep reacting at the ends, but instead "dribbles" down the inside of the silica pods and attacks the silver nanowires along the sides to yield the peapod structures.

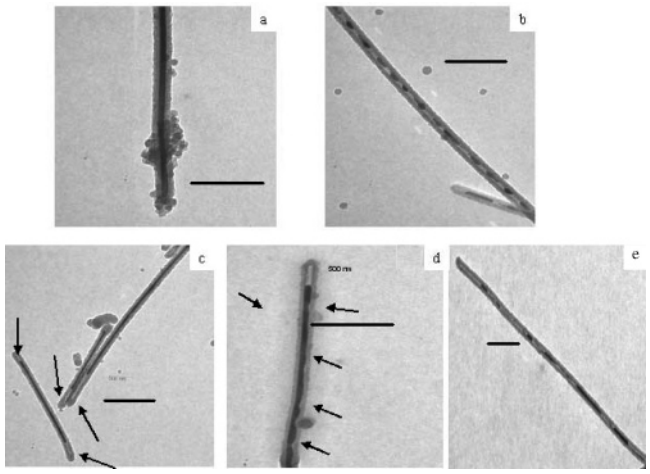

Figure 5. Transmission electron micrographs of Ag−silica assemblies under different stirring time conditions; (a) no stirring, (b) 20 min stirring, (c) 120 min stirring, (d) 240 min stirring, and (e) 360 min stirring. Scale bars: 500 nm. Arrows indicate the positions at which the dissolution reaction appears to be occurring, both at the ends of the nanowires and along their sides.

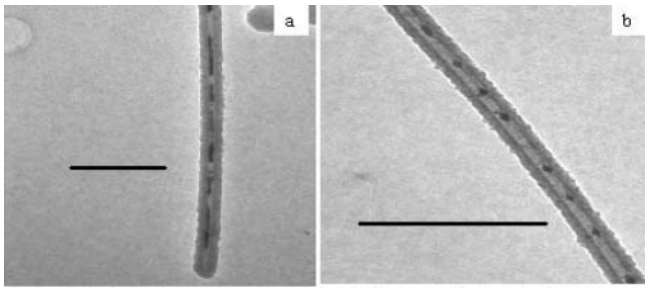

Figure 6. TEMs of representative peapod architectures obtained under conditions of incomplete dissolution of the silver when incubation time with ammonia varied from 1 day (a) to 2 days (b). Scale bar: 500 nm.

This may be in part because of the enormous excess of ammonia present; but whether there are molecular-scale "pinholes" on the silver long faces, or periodic defects that are more reactive and are manifested this way in the bulk, is completely speculative.

Reaction time is another means to tune Ag pea size and their spacings within the silica pods. A strong correlation exists between the "pea" dimensions and their spacings between the pods. As the incubation time increases, the "pea" sizes decrease and their spacings increase, respectively (Figure 6). This makes sense if, once started, the dissolution reaction proceeds on both ends of the embedded nanorod peas; as the peas shrink and reduce their aspect ratio, the interparticle distance increases.

We averaged data from a set of ∼15 experiments, with dozens of peapods per experiment, to acquire statistics on the dimensions of the peas and their spacing within the pod as a function of silica shell thickness (Figures 7, S2). Empirically, we found that the optimal reaction time for dissolution was 2 days for all sets of silica shell thicknesses after an initial stirring period of 20 min. This peculiar kinetic behavior suggests that the initial 20-min stirring allows for ammonia to diffuse through the silica shell; then the 2 days are required for the reaction that produces the complex ion and subsequent diffusion of this complex ion into solution. We have, for example, found that if, after the initial 20-min incubation with ammonia, we centrifuge out the silica-coated silver nanowires and wash them with water several times, the dissolution reaction still proceeds, suggesting that sufficient ammonia is inside the silica shell to perform the dissolution reaction.

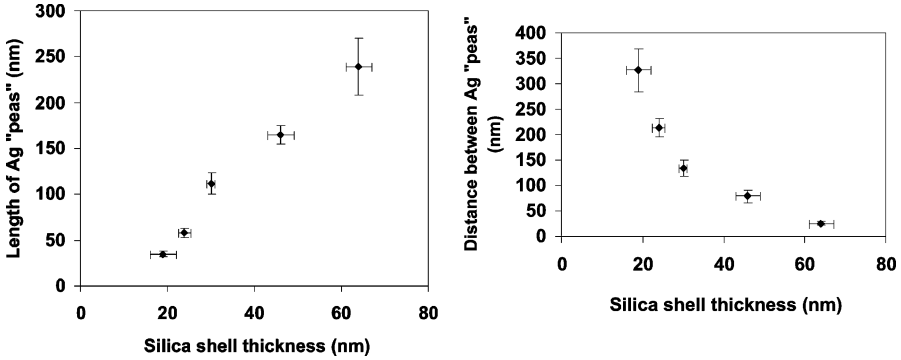

Figure 7. Plots of silver "pea" dimensions within silica pods as a function of silica shell thickness for 35 ± 2 nm initial silver nanowire diameters for two-day incubations with ammonia after a 20-min stirring period.

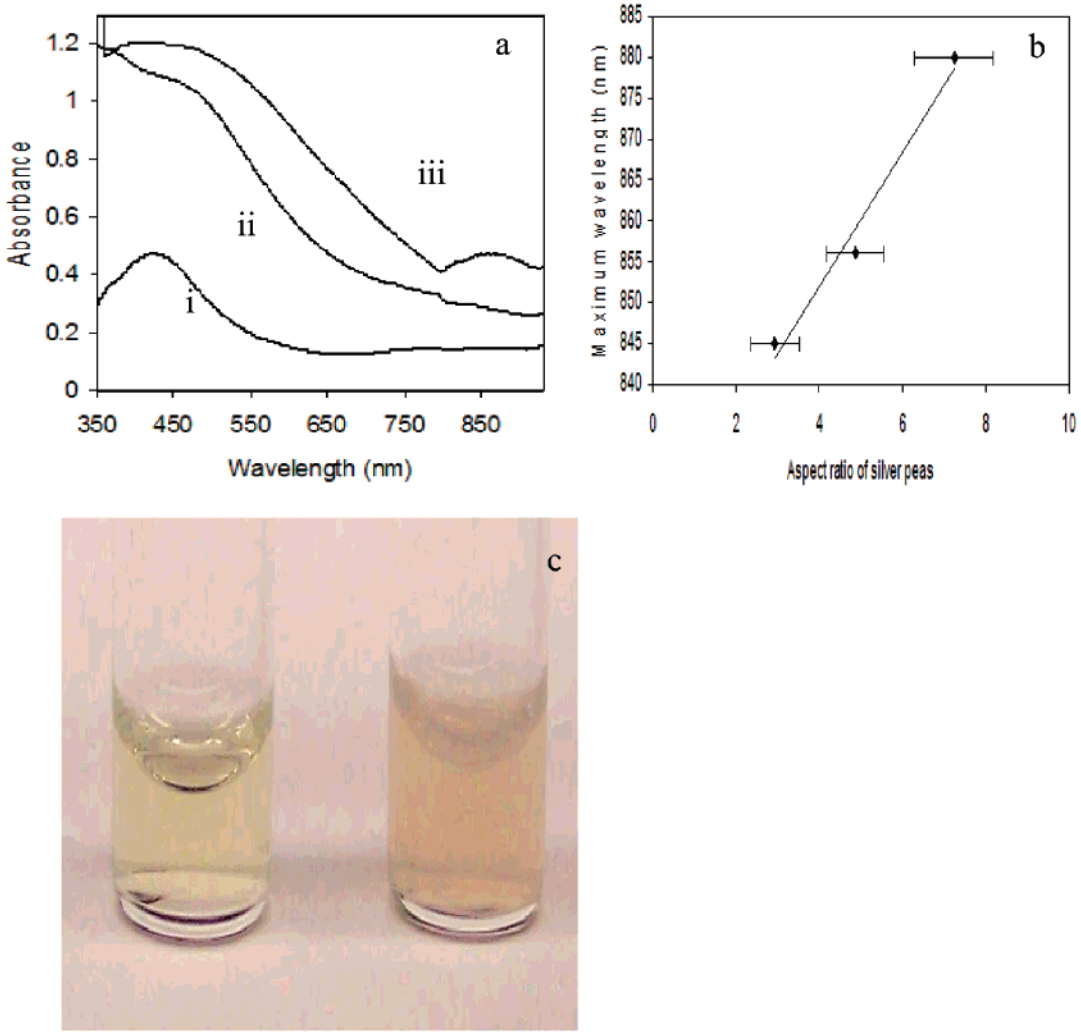

Figure 8. (a) Absorption spectra of silver nanowires (i), silver nanowires coated with SiO_2 (ii), and nanopeapods ~161 nm long by ~30 wide and spaced by ~77 nm (iii). (b) Variation of the *maximum* wavelength of nanopeapod absorbance as a function of the silver pea aspect ratio after ammonia treatment. The solid line is a linear fit to the data. (c) Photographs of aqueous solutions of Ag nanowires (left) and nanopeapods architecture (right) for 25 nm silica shell and 20 nm peas.

Ung et al. have performed analogous experiments on silica-coated silver nanospheres and investigated silver dissolution with cyanide.[22] They find, for a cyanide reaction using ~10 nm silver spheres with 15-nm-thick silica shells, that the reaction proceeds in seconds and is done in ~1 min.[22] Even for comparable shell thicknesses in our work, we find the ammonia dissolution process to be vastly slower. We interpret this to mean that diffusion through the silica shell itself is not the rate-determining step: the actual chemical reaction at the surface, in which some surface-bound species already present (e.g., possible adsorbed hydroxide from the synthesis[16]), has to be ejected in order for the Ag(0) reaction with ammonia to take place.

Optical spectroscopy of the nanopeapods does support the notion that smaller silver nanorods are indeed formed from the silver nanowires. The initial silver nanowires are pale yellow in color (Figure 8c) due to the transverse plasmon band at ~400 nm (still present in the peapod architecture) and a longitudinal band that is far out in the near-infrared and is therefore not visible to the naked eye. After reaction with ammonia, when the nanopeapods are formed, a brownish-pinkish color (Figure

8c) is observed. Spectroscopically, the presence of a new peak around 855 nm is evident and can be attributed to the longitudinal plasmon band of the "peas". As the aspect ratio of the "peas" increase, a red-shift of the longitudinal plasmon band position is observed (Figure 8b). These UV−vis absorption spectra measurements are in agreement with theory and other reported experimental results.[3,18−20]

Conclusions

Silver−silica core−shell nanowires structures were made in aqueous solution, and partial dissolution of the inner silver core with aqueous ammonia at room temperature leads to the formation of "peapod" nanoscale architectures. These structures, although still crude, resemble in principle the architectures of spaced metal nanoparticles that have the potential to be used in plasmonics and SERS-based chemical sensing. Because the method to make them is a wet-chemical one, it is amenable to scaling up. Many studies are still necessary for complete understanding of the peapod architecture systems. However, the unique size, shape, and geometry of the silver−silica nanopeapod architecture can be further refined and exploited for future applications.

Acknowledgment. We thank the University of South Carolina for funding.

Supporting Information Available: Figure showing dependence of silica shell thickness on concentration of sodium silicate precursor for various amounts of MPTMS; tables showing average pea dimensions and distances; figure showing assortment of TEMs showing silver nanowires (top), silica-coated silver nanowires. Scale bars are labeled within each micrograph. This material is available free of charge via the Internet at http://pubs.acs.org.

References and Notes

(1) (a) Xia, Y.; Yang, P.; Sun, Y.; Wu, Y.; Mayers, B.; Gates, B.; Yin, Y.; Kim, F.; Ya, H. *Adv. Mater*. **2003**, *15*, 353−389. (b) Murphy, C. J.; Sau, T. K.; Gole, A. M.; Orendorff, C. J.; Gao, J.; Gou, L.; Hunyadi, S. E.; Li, T. *J. Phys. Chem. B* **2005**, *109*, 13857−13870.

(2) (a) El-Sayed, M. A. *Acc. Chem. Res*. **2001**, *34*, 257−264. (b) Creighton, J. A.; Eadon, D. G. *J. Chem. Soc., Faraday Trans*. **1991**, *87*, 3881−3891. (c) Hu, J. T.; Odom, T. W.; Lieber, C. M. *Acc. Chem. Res*. **1999**, *32*, 435−445. (d) Link, S.; El-Sayed, M. A. *J. Phys. Chem. B* **1999**, *103*, 8410−8426.

(3) Feldheim, D.; Foss, C. A., Jr., Eds. *Metal Nanoparticles*: *Synthesis, Characterization, and Applications*; Marcel Dekker Inc.: New York, 2002.

(4) (a) Huang, Y.; Duan, X. F.; Lieber, C. M. *Small* **2005**, *1*, 142−147. (b) Fu, L.; Cao, L.; Liu, Y.; Zhu, D. *Adv. Colloid Interface Sci*. **2004**, *111*, 133. (c) Rao, C. N. R.; Deepak, F. L.; Gundiah, G. Govindaraj, A. *Prog. Solid State Chem*. **2003**, *31*, 5−147. (d) Raymo, F. M. *Adv. Mater*. **2002**, *14*, 401−414. (e) Percy, P. S. *Nature* **2000**, *406*, 1023. (f) Ito, T.; Okazaki, S. *Nature* **2000**, *406*, 1027−1031.

(5) (a) Wei, Q. H.; Su, K. H.; Durant, S.; Zhang, X. *Nano Lett*. **2004**, *4*, 1067−1071. (b) Krasavin, A. V.; Zheludev, N. I. *Appl. Phys. Lett*. **2004**, *8*, 141614−141618. (c) Brongersma, M. L.; Hartman, J. W.; Atwater, H. A. *Phys. Rev B* **2000**, *62*, R16356−R16359. (d) Quinten, M.; Krenn, J. R.; Aussenegg, F. R. *Opt. Lett* **1998**, *23*, 1331−1333.

(6) (a) Maier, S. A.; Kik, P. G.; Atwater, H. A.; Meltzer, S.; Harel, E.; Koel, B. E.; Requicha, A. G. *Nat. Mater*. **2003**, *2*, 229−232. (b) Maier, S. A.; Kik, P. G.; Atwater, H. A. *Appl. Phys. Lett*. **2002**, *81*, 1714−1716. (c) Maier, S. A.; Brongerssma, M. L.; Kik, P. G.; Atwater, H. A. *Phys. Rev B* **2002**, *65*, 193408−193412. (d) Maier, S. A.; Brongersma, M. L.; Kik, P. G.; Meltzer, S.; Requicha, A. A. G.; Atwater, H. A. *Adv. Mater*. **2001**, *13*, 1501−1505. (e) Maier, S. A.; Brongerssma, M. L.; Atwater, H. A. *Appl. Phys. Lett*. **2001**, *1*, 16−18. (f) Atwater, H. A.; Maier, S. A.; Polman, A., Dionne, J. A.; Sweatlock, L. *MRS Bull*. **2005**, *30*, 385−389.

(7) (a) Wiederrecht, G. P. *Eur. Phys. J.*: *Appl. Phys*. **2004**, *28*, 3−18. (b) Hranisavljevic, J.; Dimitrijevic, N. M.; Wurtz, G. A.; Wiederrecht, G. P. *J. Am. Chem. Soc*. **2002**, *124*, 4536−4537.

(8) (a) Schatz, G. C. *Acc. Chem. Res*. **1984**, *17*, 370−376. (b) Gersten, J. I. *J. Chem. Phys*. **1980**, *72*, 5779−5780. (c) Tao, A.; Kim, F.; Hess, C.; Goldberger, J.; He, R.; Sun, Y.; Xia, Y.; Yang, P. *Nano Lett*. **2003**, *3*, 1229−1323. (d) Jeong, D. H.; Zhang, Y. X.; Moskovits, M. *J. Phys. Chem. B* **2004**, *108*, 12724−12728. (e) Yao, J. L.; Pan, G. P.; Xue, K. H.; Wu, D. Y.; Ren, B.; Sun, D. M.; Tang, J.; Xu, X.; Tian, Z. Q. *Pure Appl. Chem*. **2000**, *72*, 221−228. (f) Nikoobakht, B.; Wang, J.; El-Sayed, M. A. *Chem. Phys. Lett*. **2002**, *366*, 17−23. (g) Nikoobakht, B.; El-Sayed, M. A. *J. Phys. Chem. A* **2003**, *107*, 3372−3378. (h) Jiang, J.; Bosnick, K.; Maillard, M.; Brus, L. *J. Phys. Chem. B* **2003**, *107*, 9964−9972. (i) Xu, H. X.; Bjerneld, E. J.; Kall, M.; Borjesson, L. *Phys. Rev. Lett*. **1999**, *83*, 4357−4360. (j) Michaels, A. M.; Jiang, J.; Brus, L. *J. Phys. Chem. B* **2000**, *104*, 11965−11971. (k) Vidal, F. J. G.; Pendry, J. B. *Phys. Rev. Lett*. **1996**, *77*, 1163−1166. (l) Wang, D.-S.; Kerker, M. *Phys. Rev. B* **1981**, *24*, 1777−1790.

(9) (a) Markel, V. A.; Shalaev, V. M.; Zhang, P.; Huynh, W.; Tay, L.; Haslett, T. L.; Moskovits, M. *Phys. Rev. B* **1999**, *59*, 10903−10909. (b) Su, K.-H.; Wei, Q.-H.; Zhang, X.; Mock, J. J.; Smith, D. R.; Schultz, S. *Nano Lett*. **2003**, *3*, 1087−1090. (c) Atay, T.; Song, J.- H.; Murmikko, A. V. *Nano Lett*. **2004**, *4*, 1627−1731. (d) Fromm, D. P.; Sundaramurthy, A.; Schuck, P. J.; Kino, G.; Moerner, W. E. *Nano Lett*. **2004**, *4*, 957−961. (e) Enoch, S.; Quindant, R.; Badenes, G. *Opt. Express* **2004**, *12*, 3422−3427. (f) Ghenuche, P.; Quindant, R.; Badenes, G. *Opt. Lett*. **2005**, *30*, 1882−1884. (g) Orendorff, C. J.; Gole, A.; Sau, T. K.; Murphy, C. J. *Anal. Chem*. **2005**, *77*, 3261−3266. (h) Orendorff, C. J.; Gearheart, L.; Jana, N. R.; Murphy, C. J., *PhysChemChemPhys* **2006**, *8*, 165−170.

(10) Zou, S. L.; Schatz, G. C. *Chem. Phys. Lett*. **2005**, *403*, 62−67.

(11) Wei, Q.-H.; Su, K.-H.; Durant, S.; Zhang, X. *Nano Lett*. **2004**, *4*, 1067−1071.

(12) (a)Yin, Y.; Lu, Y.; Gates, B.; Xia, Y. *J. Am. Chem. Soc*. **2001**, *123*, 8718−8729. (b) Alivisatos, A. P.; Johnsson, K. P.; Peng, X. G.; Wilson, T. E.; Loweth, C. J.; Bruchez, M. P.; Schultz, P. G. *Nature* **1996**, *382*, 609−611. (c) Claridge, S. A.; Goh, S. L.; Frechet, J. M.; Williams, S. C.; Micheel, C. M.; Alivisatos, A. P. *Chem. Mater*. **2005**, *17*, 1628−1635.

(13) Ebbesen, T. W.; Hiura, H.; Bisher, M. E.; Treacy, M. M. J.; ShreeveKeyer, J. L.; Haushalter, R. C. *Adv. Mater*. **1996**, *8*, 155−158.

(14) Dujardin, E.; Peet, C.; Stubbs, G.; Culver, J. N.; Mann, S. *Nano Lett*. **2003**, *3*, 413−417.

(15) Sioss, J. A.; Keating, C. D. *Nano Lett*. **2005**, *5*, 1779−1783.

(16) Caswell, K. K.; Bender, C. M.; Murphy, C. J. *Nano Lett*. **2003**, *3*, 667−669.

(17) (a) Hu, M.; Noda, S.; Okubo, T.; Yamaguchi, Y.; Komiyama, H. *Appl. Surf. Sci*. **2001**, *181*, 307−316. (b) Huang, X.; Huang, H.; Wu, N.; Hu, R.; Zhu, T.; Liu, Z. *Surf. Sci*. **2000**, *459*, 183−190. (c) Kulinowski, K. M.; Jiang, P.; Vaswani, H.; Colvin, V. L. *Adv. Mater*. **2000**, *12*, 833−838. (d) Fang, M.; Kim, C. H.; Martin, B. R.; Mallouk., T. E. *J. Nanopart. Res*. **1999**, *1*, 43−48.

(18) (a) Obare, S. O.; Jana, N. R.; Murphy, C. J. *Nano Lett*. **2001**, *1*, 601−603. (b) Mine, E. M.; Samada, A.; Kobayashi, Y.; Konno, M.; Liz-Marzán, L. M. *J. Colloid Interface Sci*. **2003**, *264*, 385−390. (c) Chen, M. M.; Katz, A. *Langmuir* **2002**, *18*, 8566−8572; (d) Santra, S.; Zhang, P.; Wang, K.; Tapec, R.; Tan, W. *Anal. Chem*. **2001**, *73*, 4988−4993. (e) Bhattacharyya, S.; Saha, S. K.; Chakravorty, D. *Appl. Phys. Lett*. **2000**, *77*, 3770−3772. (f) Liu, S.; Yue, J.; Gedanken, A. *Adv. Mater*. **2001**, *9*, 656−658.

(19) Liz-Marzán, L. M.; Giersig, M.; Mulvaney, P. *Langmuir* **1996**, *12*, 4329−4335.

(20) (a) Kobayashi, Y.; Katakami, H.; Mine, E.; Nagao, D.; Konno, M.; Liz-Marzán, L. M. *J. Colloid Interface Sci*. **2005**, *283*, 392−396. (b) Yin, Y; Lu, Y.; Sun, Y.; Xia, Y. *Nano Lett*. **2002**, *2*, 427−430.

(21) Link, S.; Mohamed, M. B.; El-Sayed, M. A. *J. Phys. Chem. B* **1999**, *103*, 3073−3077.

(22) Ung, T.; Liz-Marzán, L. M.; Mulvaney, P. *Langmuir* **1998**, *14*, 3740−3748.